Interictal EEG Discoordination in a Rat Seizure Model

Samuel A. Neymotin, Heekyung Lee,† André A. Fenton,*†‡§ and William W. Lytton*†‡‖*

Abstract: Cognitive and psychiatric comorbidities are common and clinically important in medial temporal lobe epilepsy and are likely caused by ongoing abnormalities in brain activity. In addition, it is unclear how the dynamics of interictal brain activity in medial temporal lobe epilepsy contributes to the generation of seizures. To investigate these issues, the authors evaluated multisite interictal EEG from a perinatal excitotoxic, hippocampal lesion rat model of medial temporal lobe epilepsy. Sample entropy, an information theoretical measure, demonstrated decreased complexity at different time scales and across all channels in epileptic animals. However, higher-order multiarea measures showed evidence of increased variability in population correlation measures. This apparent paradox was resolved by noting that although the EEG from epileptic animals was overall more stereotyped, there were frequent periods where two or more brain areas "broke off" from ongoing brain activity in epileptic animals, producing decorrelations between areas. These decorrelations were particularly apparent across the midline, suggesting impairments of interhemispheric coordination, a form of interhemispheric diaschisis. Both the observed alterations could contribute to a reduction in brain functionality: an overall reduction in complexity and a failure of interhemispheric brain coordination, suggesting a breakdown in communication between hemispheres. The authors speculate that any tendency of areas to lose communication or break away from coordinated brain activity might predispose to seizures in these areas.

Key Words: Epilepsy, Seizure, Interictal, Coordination, Synchronization.

(*J Clin Neurophysiol* 2010;27: 438–444)

Recently, a diverse range of methods have been applied to the analysis of EEG activity from patients with medial temporal lobe epilepsy (MTLE) (Kramer et al., 2008; Ossadtchi et al., 2010; Usui et al., 2010). There are a number of results that suggest ongoing interictal brain abnormalities in the epileptic brain (Hermann et al., 2009). However, further study is required to provide a better understanding of ongoing dynamic alterations during these interictal periods. This has been somewhat difficult to demonstrate, in part, due to the lack of detailed, long-term multisite electrocorticographic recordings in patients.

Prior studies have demonstrated that there is a loss of complexity in interictal EEG time series (Weber et al., 1998) and, more generally, that the complexity of many biologic signals is reduced with disease or with aging (Costa et al., 2002; Goldberger et al., 2002). Techniques from information theory have been used to quantify the entropy of EEG activity under anesthesia (Li et al., 2008) and to measure the entropy of various physiological time series using approximate and sample entropy (Richman and Moorman, 2000). These information theoretical measures have been able to link brain dynamical activity with clinical differences.

To examine underlying dynamical relations across brain areas, we studied a rat MTLE model produced through excitotoxic lesioning of bilateral ventral hippocampus in the neonatal animal. We examined multisite data from prolonged recordings to assess alterations in dynamical signature during interictal periods. Ictal periods were removed using the White-Dudek-Staley (WDS) seizure detection algorithm (White et al., 2006) that is parameterized for high sensitivity and low specificity. The entropy measure we used works on a single dimension and therefore cannot measure higher-dimensional alterations involving interactions across channels. Therefore, we complemented this entropy technique with multisite correlation measures. Using these measures, we found evidence for abnormalities in interregional coordination in the interictal epileptic brain.

METHODS

Animal Model

Timed-pregnant Long-Evans rats were obtained at 13 to 14 days of gestation from Charles River Laboratories (Wilmington, MA). The pups were lesioned according to the procedure adapted from Lipska et al. (1993). On postnatal day 7 (P7), pups weighing 14 to 18 g were anesthetized by hypothermia (placed on ice for 15–20 minutes). A puncture hole was made bilaterally on the skull for injection sites (relative to bregma AP: −3.0 mm, ML: +3.5 mm), and 0.3 μL of ibotenic acid solution (IBO, 10 μg/μL, Sigma) or saline (SAL, control rats) was infused bilaterally into the ventral hippocampal formation (relative to the skull surface DV: −5.0 mm) at 0.15 μL/min. The pups were warmed and then returned to their mothers. On P21, animals were weaned.

EEG and Local Field Potential Recording

Between P60 and P90, nine IBO-lesion and seven SAL-control rats were implanted and recorded for local field potentials [procedure adapted from Olypher et al. (2006) and EEG procedure adapted from Zhong et al. (2009)]. Electrodes were made by attaching 75-μm Nichrome wire to contacts in Mill-Max connectors for local field potential recordings, and a stainless steel jeweler's screw on the rat's skull was attached to a Mill-Max connector by a 75-μm Nichrome wire for epidural cortical EEG recordings. Recordings were made bilaterally from the following locations: piriform cortex^{w}: AP: −0.9, ML: +5.5, DV: 8.8; amygdala: AP: −2.8, ML: +4.8, DV: 8.8; entorhinal cortex: AP: −6.7, ML: +4.7, DV: 6.8; thalamus: AP: −3.6, ML: +1.0, DV: 5.5; mPFC: AP: +3.0, ML: +1.0, DV: 4.0; dorsal hippocampus^{w}: AP: −4.0, ML: +2.5, DV: 3.0; ventral hippocampus: AP: −5.6, ML: +4.5, DV: 3.5; frontal screw^{w}: AP: 0, ML: +3.0; back screw^{w}: AP: −6.0, ML: +3.0 (all in millimeter; superscript *w* indicates the eight electrodes in animals used for Figs. 2–4). All electrodes were referred to a reference

From *SUNY Downstate/Poly-NYU Joint Biomedical Engineering Program; †Neural and Behavioral Science Program; Departments of ‡Physiology & Pharmacology and §Neurology, SUNY Downstate, Brooklyn; and ‖Center for Neural Science, New York University, New York, New York, and the Department of Neurology, Kings County Hospital Center, Brooklyn, New York.

Supported by National Institute of Mental Health (R01MH084038) and National Institute of Neurologic Disorders and Stroke (R42NS064474).

Address correspondence and reprint requests to William W. Lytton, 450 Clarkson Ave., Box 31, Brooklyn, NY 11203-2098; e-mail: billl@neurosim.downstate.edu.

ISSN: 0736-0258/10/2706-0438

electrode implanted in the cerebellar white matter. Rats were recorded in their home cages for 1 hour at a time for a total of 12 to 15 hours. Sixteen-channel, 12-channel, or 8-channel recordings of electrophysiological signals were performed. For the 12- and 16-channel recordings, the signals were digitized (24 bits, 48 kHz; Axona Ltd., St. Albans, UK) and transmitted galvanically along a counter-balanced cable. For the 8-channel recordings, the signals were digitized (24 bits, 12 kHz) and transmitted wirelessly (Bio-Signal Group Corp., Brooklyn, NY). In the 8-, 12-, and 16-channel systems, the digital signals were received by a set of dedicated digital signal processors, bandpass filtered (1–500 Hz), amplified digitally, and then downsampled (2000 Hz).

Algorithms and Software

To compare interictal EEG/local field potential (hereafter called simply EEG), we detected and excluded both seizures and high-amplitude, stereotyped noise using the WDS algorithm that is described here briefly (White et al., 2006). The algorithm detected seizures (or sometimes noise) based on two criteria: (1) the number of spikes (assessed by high first derivative); and (2) correlations between minimum and maximum values in 2-second windows.

The spikes were detected by requiring at least n successive values in the time series to be monotonically increasing. In addition, the sum of the difference in values of the successively increasing samples had to surpass a threshold, th.

The first step in calculating the correlation-based measure was finding minimum and maximum values in all the 2-second windows. Next, a metric was calculated that used the following values for each 2-second window: $HV_i = MIN[max_i, MAX(max_{i+1}, max_{i+2})]$, $LV_i = MAX[min_i, MIN(min_{i+1}, min_{i+2})]$. Here, max_i and min_i denote the maximum and minimal value in 2-second window *i.* The metric was then defined as $M_i = HV_i - LV_i$ and was calculated for each 2-second window, except for the last two windows in the time series. This metric measures the overlap in the range of period *i* with the next two periods, $i + 1$ and $i + 2$. It is useful for seizure detection because spikes in a seizure tend to have similar, correlated ranges, and during nonseizure periods, this type of activity is absent. This is shown clearly in Fig. 3 of White et al. (2006).

Once the metric was calculated, each 12-second window was assigned the sum of metric values calculated from each of its 2-second subwindows. For any 12-second window to qualify as a seizure period, both the spike count and correlation measures had to surpass a threshold.

Before running the seizure detection algorithm, we downsampled our digitized signals from 2 kHz to 100 Hz using a 10-millisecond moving average filter. This was done to avoid noise-related fluctuations that would discredit spikes where a single sample over a 0.5-millisecond interval did not increase monotonically. We also avoided extra calculations by not rectifying the signal [unlike the WDS algorithm as described in White et al. (2006)] because all our spikes were in the upward direction.

The algorithm's parameters (thresholds) were set to increase sensitivity (reduced specificity) so as to try to eliminate all seizures. Although the WDS algorithm works on a single channel at a time, we increased sensitivity further by considering all time intervals that had seizures from at least one channel detected on them as seizures.

After cutting out the seizures, we analyzed the remaining interictal activity. To determine the complexity of the EEG time series, we calculated the sample entropy (SampEn) that is defined as $\text{SampEn}(m,r,N) = -\ln\frac{A(m)}{B(m-1)}$ (Lake et al., 2002; Richman and Moorman, 2000). SampEn is the negative natural logarithm of an estimate of the conditional probability that subseries (epochs) of length $m - 1$ that match pointwise within a tolerance r also match at the mth point. In the equation, $A(m)$ and $B(m - 1)$ are the number of subseries of length m and $m - 1$, respectively, that match within a tolerance of r. Points within the subseries X and Y are said to match if the corresponding elements, X_i and Y_i, have a difference less than r. The subseries are taken from different times within the portion of the time series under analysis. SampEn measures variability of a time series by determining how likely the $m + 1$th point is to match, given that the past m points match. For highly regular signals, SampEn will be low and for complex signals high. We ran SampEn on downsampled signals using a moving average with a window size of 10 milliseconds to reduce noise. Based on previous work, we used a tolerance parameter, r, of 0.2 times the signal's standard deviation and an epoch length, m, of two samples, which corresponded to 20 milliseconds in the downsampled signal. We used 12 seconds of the time series at a time, resulting in the number of points analyzed by SampEn at a time to be $N = 1200$. We tried different window sizes in the moving average filter, as suggested by multiscale analysis methods (Costa et al., 2002) and obtained similar results. We examined recordings from all 16 rats across three different electrode configurations. We summed SampEn across channels to produce the histograms shown in Fig. 1.

To determine activity coordination across brain areas, we used methods to denote population correlation (PCorr) and population coordination (PCo). PCorr is a vector of all $\frac{n(n-1)}{2}$ pairs (28 here from the eight channels), pairwise Pearson correlation values

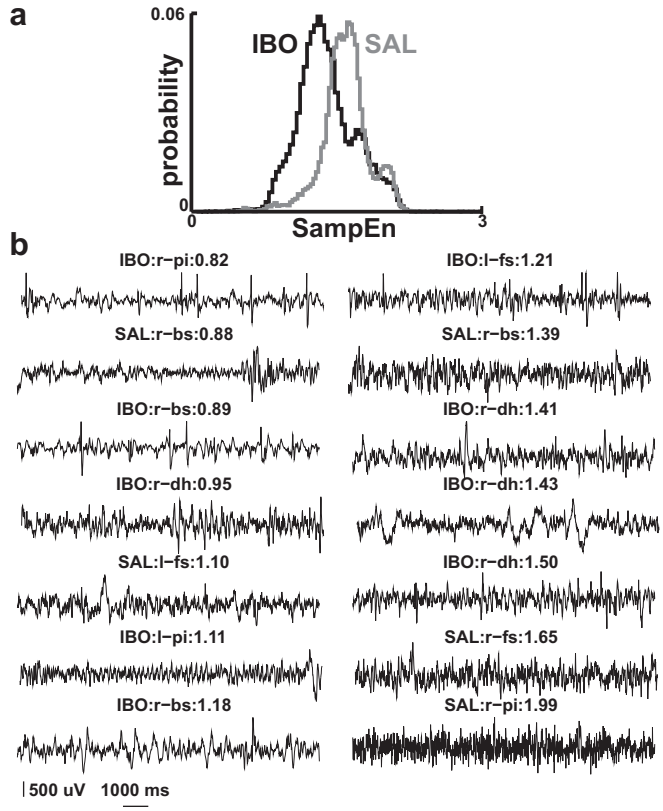

FIGURE 1. Entropy differs between groups. **a**, Sample entropy values for all animals across all channels (12-second windows). The epileptic animals (IBO) have significantly lower entropies than controls (SAL) ($P < 0.0001$). **b**, Example traces of 12 seconds of activity from indicated groups and electrode locations, sorted by increasing entropy values (given after second colon).

taken over each 1-second interval. Pearson correlation is defined between two vectors or time series, X, and Y as $r = \frac{\sum_{i=1}^{n}(X_i - \bar{X})(Y_i - \bar{Y})}{\sqrt{\sum_{i=1}^{n}(X_i - \bar{X})^2}\sqrt{\sum_{i=1}^{n}(Y_i - \bar{Y})^2}}$.

A PCorr vector thereby captures the correlations across all areas during a 1-second "instant." We display this vector in a redundant 8 × 8 matrix format for clarity of presentation. To determine the similarity of these PCorr vectors across time, we took Pearson correlations between all pairs of PCorr vectors over periods of up to 3 hours of continuous recording. The resulting correlation matrix is called population coordination (PCo), where the x and y axes are t_0 and t_1 times with matrix entries giving correlation between PCorr vectors at those times. Movement away from the diagonal then represents time passage away from a given time, and recurrence of similar PCorr vectors appears as bright spots on the matrix (Fig. 4a).

Software used for analysis was run in the NEURON simulation environment with the Neural Query System data-mining system (Carnevale and Hines, 2006; Lytton, 2006). We also used the Matlab function princomp for principal components analysis (The MathWorks Inc., 1998). Analysis software enhancements used here are available on SimToolDB (http://senselab.med.yale.edu/simtooldb).

RESULTS

Evaluation was done from intracortical recordings from 16 animals subjected to neonatal ventral hippocampal injection of either saline (SAL, control) or ibotenic acid (IBO). Animals with IBO injection suffered several electrographic seizures each day, generalized spike-and-wave on EEG, occasionally associated with behavioral manifestations. Each animal had 1 to 12 recordings with 8, 12, or 16 channels. Average recording duration was 47 minutes. Because we were interested in studying baseline activity, we preprocessed the signals to get rid of seizures using the WDS algorithm introduced by White et al.(2006), leaving us with 25.2 hours of recording after removing seizures (236.8 hours of data across all channels). For a more detailed analysis in Figs. 2 to 4, we reduced our focus to four animals (two epileptic and two control), which had prolonged recordings using a single 8-channel montage (16.8 hours of recording; 134.4 hours total data across all channels after preprocessing).

Reduced Interictal Entropy in Epileptic Animals

We measured incoordination of the EEG signals using sample entropy (SampEn) across all individual channels (Fig. 1a). Entropy was larger for control animals than for epileptic animals, consistent with the general hypothesis that reduction in the entropy of biologic signals is associated with disease and aging (Costa et al., 2002; Goldberger et al., 2002; Weber et al., 1998). These entropy differences were observed in time ranges on the order of 20 milliseconds, consistent with the period of gamma oscillations, which have been proposed for involvement in cognitive function and synchronization (Olypher et al., 2006; Uhlhaas and Singer, 2006; Zhong et al., 2009). The small right side peak seen on both histograms reflected sensitivity of the algorithm to oscillation near the time scale used for the analysis. Interestingly, the entropy curve for the epileptic animals showed a hint of left side shoulder, consistent with an excess of low-entropy stereotyped signal, which could be due to additional brief seizure activity not picked up by the WDS algorithm. Example traces with increasing levels of entropy are shown (Fig. 1b). Traces with lower entropy were more stereotyped in appearance and appeared to show a narrowing of frequency content.

Alterations of EEG entropy across channels may be a combination of incoordination within each area and incoordination across areas. Sample entropy cannot help us distinguish these possibilities because it is a single channel measure that does not reflect simultaneous activity across channels. We hypothesized that the hippocampal lesions would not only alter hippocampal activity but also damage coordination across areas, whether or not those areas still produced normal activity intrinsically. To assess this possibility, we used a population correlation measure that could capture high-dimensional interareal incoordination.

Population Correlations Across Brain Areas

We built population correlation (PCorr) matrices by looking at all nontrivial (nonself) correlation pairs across the eight channels (Fig. 2a). Each matrix shows how the channels relate to each other during a particular 1-second period. On average, the PCorr matrices for epileptic animals showed a reduction of correlation across the midline compared with ipsilateral correlations and compared with controls, including a substantially higher probability of negative correlations (Figs. 2a and 2b). Figure 2b also suggested a somewhat lower correlation of activity of areas within the left hemisphere in epileptic animals.

Two individual 1-second periods are shown in Fig. 2c. The epileptic animals had greatly reduced correlation across hemispheres (darker regions in top left and lower right), as well as lower correlations within left hemisphere (lower left) and within right hemisphere (upper right). This type of pattern was seen far more often in the epileptic animals. As in this example, traces from the epileptic animal typically exhibited more high-amplitude, out-of-phase activity. Here, this was seen particularly in the out-of-phase peaks of the left piriform (l-pi) and right back cortical screw (r-bs) traces. In contrast, the activity in the control animal traces showed typical, uniformly intermediate to high positive correlations within the hemispheres, with only slightly lower correlations across hemispheres.

To better visualize the differences between epileptic and control animals, we handled each PCorr matrix as a 28-dimensional PCorr vector (the 8 × 8 matrix without the diagonal and without the redundancy across the diagonal). We then reduced the dimensionality from 28 to 2 using principal component analysis (Fig. 3). Control vectors were more tightly clustered than those of the epileptic animals. Although there is overlap between the projections of the two groups, the clusters can be readily distinguished, suggesting distinct dynamical relationships within each group. Together with Fig. 2, this supports the conclusion that some of this variability is due to alterations in the relations between areas.

Figure 3b shows PCorr matrices and data traces associated with selected points in regions of interest. S1 and S2 were typical vectors from the control animals, both with low values of principal component 1 (PC1) and moderate values of PC2. Both these PCorr matrices had fairly high correlation between the different brain areas. I1 (from epileptic animal) was from a region of principal component analysis space that overlaps with that of the control animals. The values in the PCorr matrix also showed high correlation between the different areas. However, I1 showed a notably low level of correlation between the left dorsal hippocampus (l-dh) and structures in the right hemisphere. Although the overlap suggested that control and epileptic animals showed similar interareal relations, movement along PC1 resulted in substantial change in correlation state. I2, from a region mostly occupied by epilepsy animal vectors, showed high-amplitude, slow activity in the right front cortical screw (r-fs) and right piriform cortex (r-pi), as well as other structures in the right hemisphere. This activity was poorly correlated with activity elsewhere in the brain, particularly in the other hemisphere. Such out-of-phase patterns were commonly seen in the

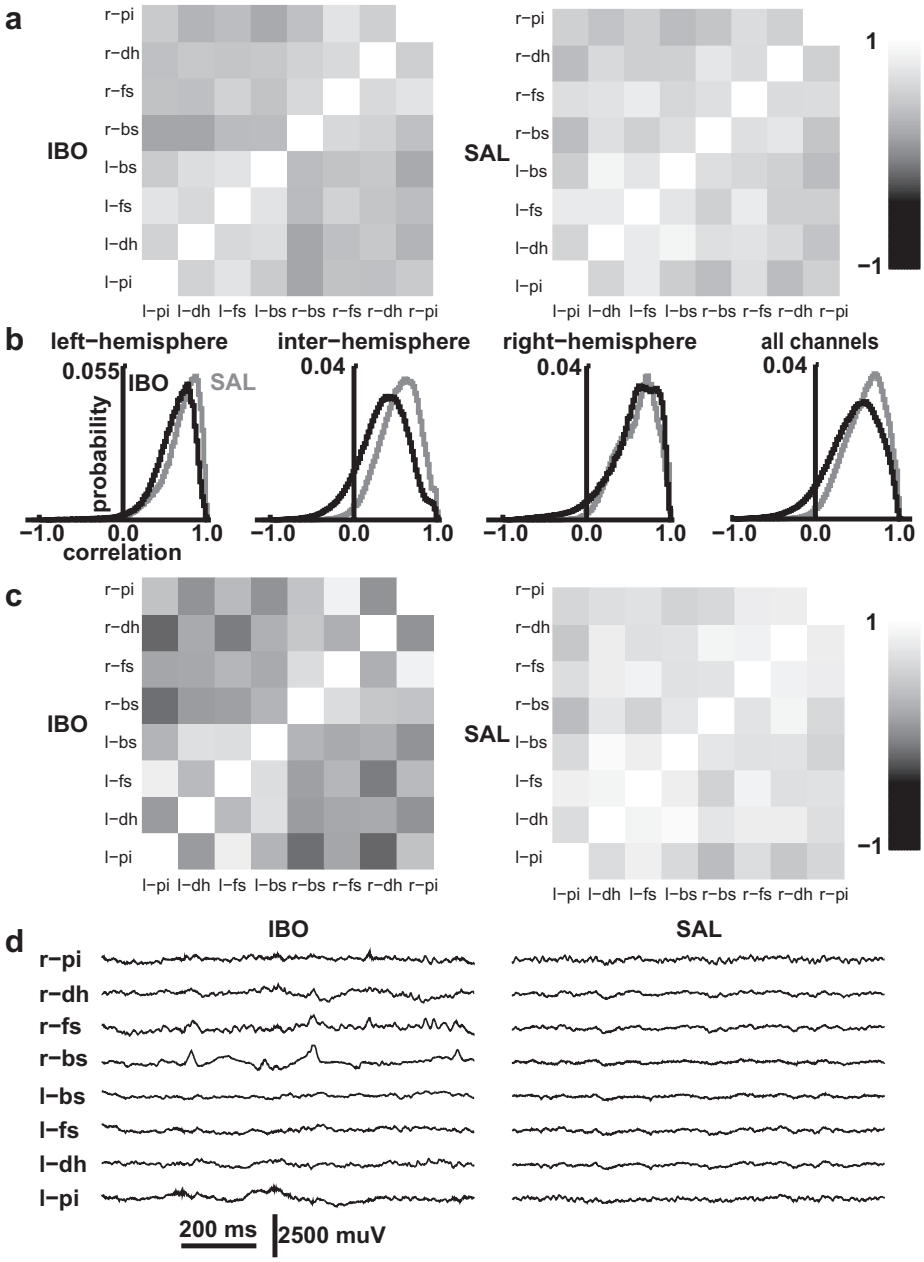

FIGURE 2. Reduced interhemispheric activity coordination in epileptic animals. **a**, Average PCorr matrices from epileptic (left) and control (right) animals show more dark (uncorrelated) pairs for epileptic animals. **b**, Histograms of values in PCorr matrices on channel pairs confirm this overall correlation shift and demonstrate that it is primarily interhemispheric. Black histogram: epileptic; gray: control. **c**, Individual examples of PCorr matrices for an epileptic (left) and control (right) animal. Note the darkening of the interhemispheric quadrants (upper left and lower right) for the epileptic animal. **d**, Traces corresponding to PCorr matrices above.

epileptic animals but rarely in the controls. I3 had a PCorr matrix demonstrating high correlation between the right piriform cortex (r-pi) and right dorsal hippocampus (r-dh), both of which had negative correlations with most other areas but weak positive correlation with the left piriform cortex, again due to high-amplitude, slow activity. In addition, I3 showed low correlation between the left piriform cortex (l-pi) and the other channels in the left hemisphere and most of the other channels in the right hemisphere. A notable feature in I3 is the very high correlation between the remaining areas in the left and right hemisphere, suggesting organization within a subset of areas, which then may be dynamically isolated from other areas. Such combinations of high positive and high negative correlations are far less likely to occur in the control animals, as evidenced by the lack of control points in these outlier regions.

Assessment of Variability in Time

The PCorr analysis demonstrated that changes in relationships across brain regions was one aspect of the changes in variability demonstrated by the entropy measures (Fig. 1). We complemented this assessment of spatial variability by looking for temporal variability in the Population Correlation (PCorr) vectors, assessing Pearson correlations across time to produce a Population Coordination (PCo) measure. High correlations in the PCo matrix demonstrate recurrence in time of particular spatial correlation patterns.

Figure 4 shows the different patterns of brain-state recurrence in a 16.5-minute period from a control compared with an epileptic animal. The PCo control shows consistent levels across time, without long periods of highs (strong self-similarity) or lows (dissimilarities). By contrast, the epileptic animal PCo matrix shows dark

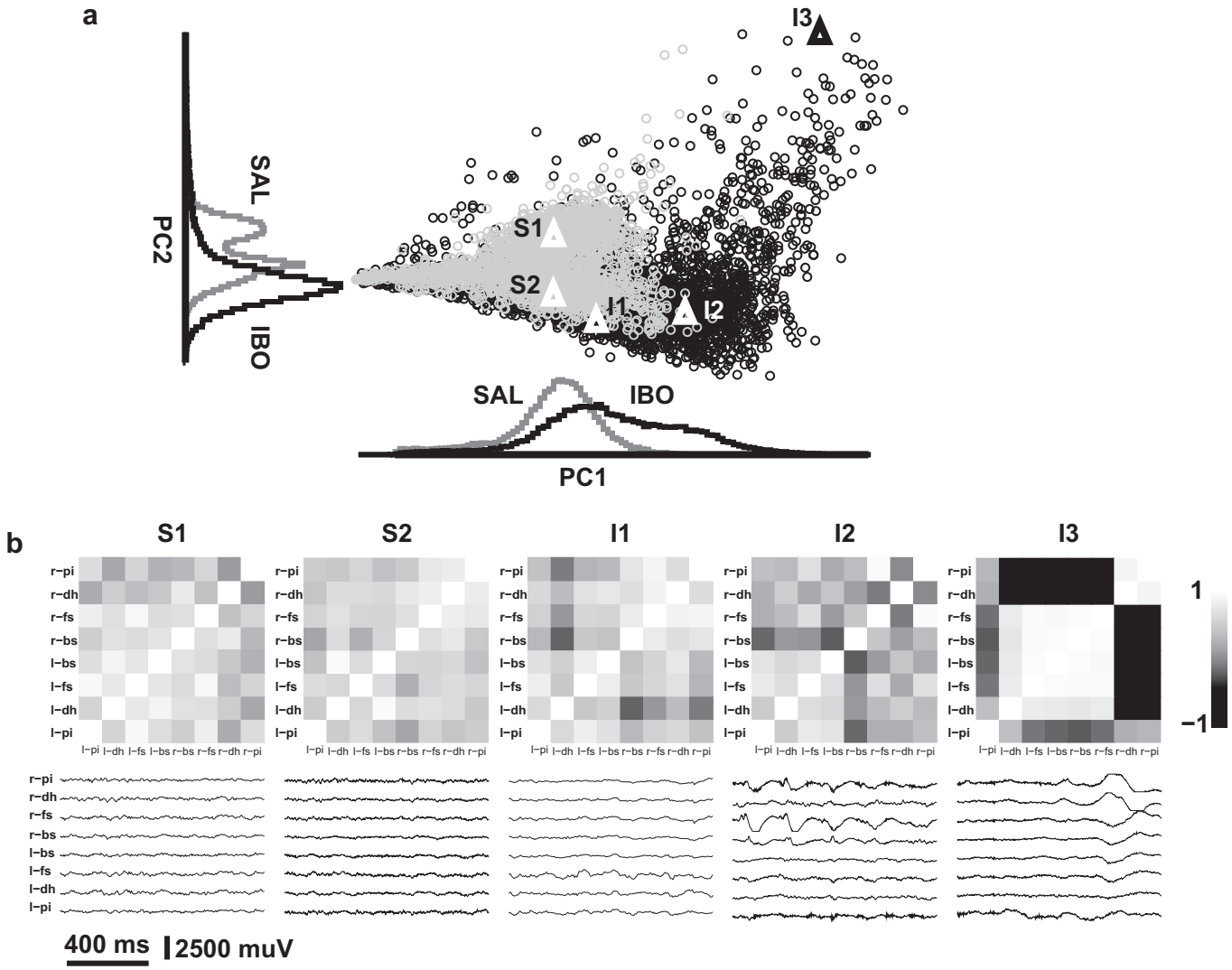

FIGURE 3. Principal component (PC) projections of PCorr vectors for epileptic (IBO, I) and control (SAL, S) animals. **a**, PC1, PC2. 10% of data randomly chosen for display; gray points, control; black, epileptic. Examples given by large triangles are shown in (**b**) with PCorr on top and raw traces below.

stripes where significant negative correlations are present, signifying anomalous states that have little similarity with most other periods. For example, the PCorr on the left of Fig. 4c is part of a 20-second period of similar anomalous activity at ~7 minutes that recurs at later times (multiple white spots on vertical line above diagonal). Overall, the epileptic animals have a greater number of low correlations across time, with values that venture into the negative range (Fig. 4b).

However, this result could be predicted from Fig. 3: the epileptic animals' PCorrs occupy more of the high-dimensional space, so there is more possibility for decorrelation across time. Therefore, we ran a shuffle test (IBO-shuf for epileptic and SAL-shuf for control animal) that also showed a substantial shift. The question of temporal variability must be regarded as unresolved, because the histogram of matrix values is too reduced a representation of the complexity of the PCo matrix to address the temporal variability hypothesis with confidence using this technique.

In Fig. 4c, the PCorr on the left represents the anomalous brain-state that produced the dark vertical line above the asterisk in Fig. 4a. Examination of this PCorr matrix revealed high positive correlation between right piriform cortex and dorsal hippocampus with negative correlations between these structures and the rest of the brain. This highlights a common pattern in the epileptic animals whereby a pair of structures appeared to be linked with high-amplitude, slow activity and be somewhat isolated from activity elsewhere in the brain. In particular, piriform cortex and dorsal hippocampus were often coordinated in this way. In contrast, the more typical pattern at the right of Fig. 4c, corresponding to the asterisk on the *y* axis, showed low-amplitude activity levels with less decorrelation across areas. However, even this fairly typical pattern for the epileptic animals had a notable level of low correlation between right back cortical screw (r-bs) and the activity on most other channels.

DISCUSSION

We have demonstrated differences in the dynamics of EEG activity during the interictal state in an animal model of MTLE. The

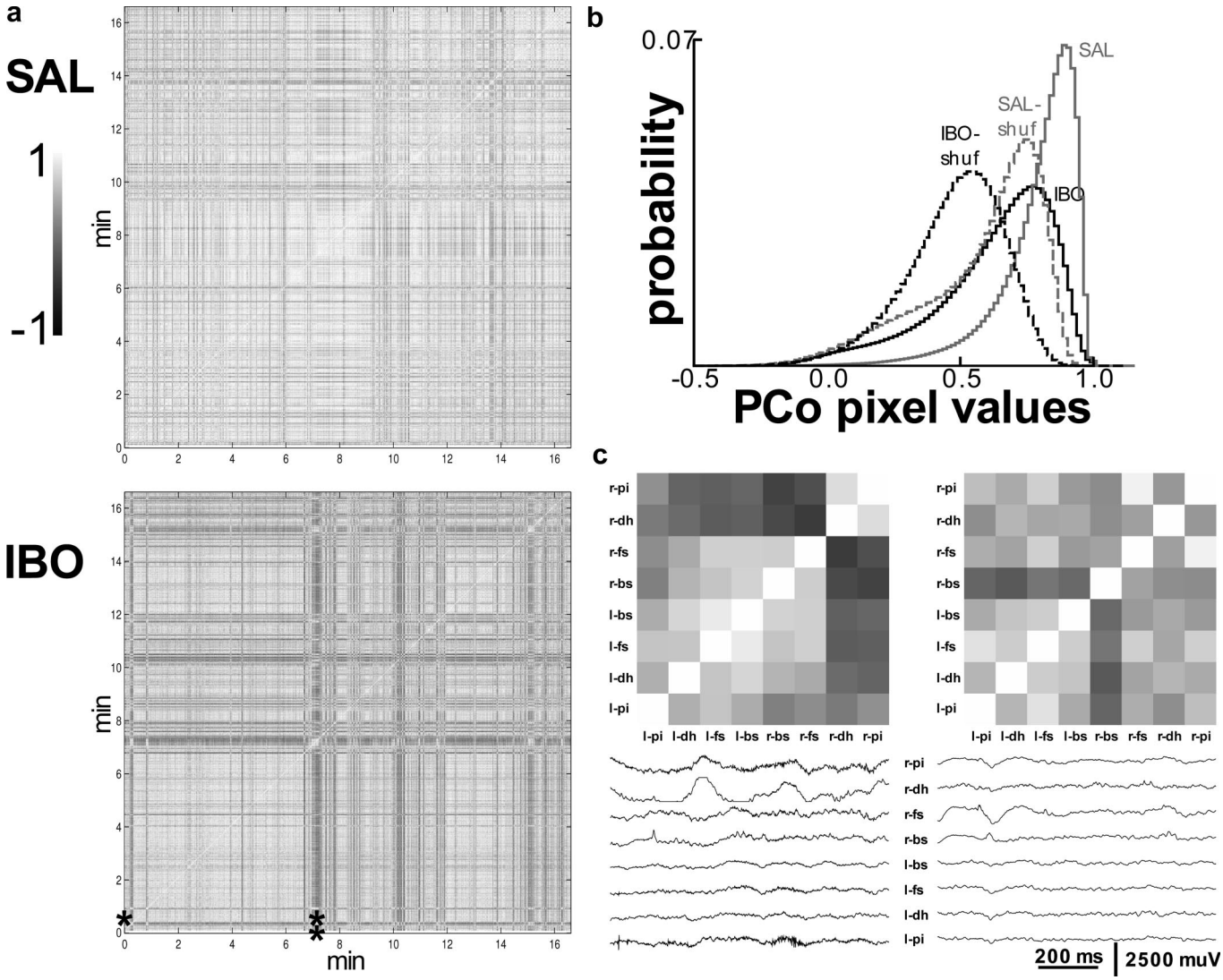

FIGURE 4. Decorrelation of activity across time in epileptic animals. PCo of 16.5 minutes duration from control (SAL) and epileptic (IBO) animals. **b**, Summary of time correlations across full 16.8 hours dataset. Epileptic animals showed more low and negative correlation values but significance unclear: we also see a shift using shuffled vectors (IBO-shuf, SAL-shuf). **c**, Two PCorr matrices and associated traces pulled out from point in PCo denoted by asterisks (left PCorr from 7 minutes 10 seconds; right PCorr from 33 seconds). PCorr on left correlates poorly with most, but not all, other times: this can be seen by noting dark vertical line with white spots above asterisk pair at 7 minutes 10 seconds in bottom of panel (**a**).

epileptic animals had substantially lower entropy of their EEG signals. This has previously been shown to be the case in interictal states and relates to pathology and disease in biologic systems (Weber et al., 1998; Widman et al., 2000). The lower entropy is evidence of reduced complexity in the signals. However, our PCorr measure demonstrated a broader distribution of vectors in the epileptic animals. Although this could be interpreted as consistent with greater dynamic complexity, further analysis revealed that this complexity occurred due to portions of the brain showing high-amplitude, slow activity that was independent of activity elsewhere. Hence, this is a pathologic complexity resulting from discoordination or deranged coordination across areas. The discoordination does not indicate that there is no correlation between activity in the different areas but instead demonstrates an alteration in activity dynamics and unusually low or negative levels of activity correlation between regions. This implies that brain regions are still interacting but in an altered, presumably pathologic, way.

The observed discoordination was particularly pronounced across the midline, suggesting a failure of interhemispheric coordination, a form of interhemispheric diaschisis (Feeney and Baron, 1986; Kempinsky, 1958; Meyer et al., 1993). Interestingly, we previously observed a similar interhemispheric effect with alterations in single unit discharge of pyramidal neurons in one hippocampus after temporary inactivation of the other (Olypher et al., 2006).

The term diaschisis was coined by von Monakow (1914) to describe reduced activity in an area receiving excitatory projections from a damaged area of brain. Over the past century, the term has broadened to include all remote effects of damage, and it has been recognized that dynamic neurogenic as well as vasogenic/chemical

factors likely contribute to the phenomenon (Meyer et al., 1993). For example, interhemispheric diaschisis may involve complex dynamical interactions reflecting disruption in callosal projections that likely have a substantial feedforward inhibitory component (Reggia et al., 2001). From this perspective, it seems reasonable to further extend the term to the present circumstance, where an initial perinatal ablation propagates dynamical disorder through development to produce a situation where brain interrelations are chronically disorganized. The initial damage here is to bilateral ventral hippocampus. The areas that seemed most prone to dynamical disconnection from the rest of the brain were dorsal hippocampus and possibly piriform cortex (see I2 and I3 in Fig. 3; this remains to be examined more closely). Dorsal hippocampus seems likely to directly show diaschisis, given the close interactions between ventral and dorsal hippocampus (Olypher et al., 2006). The origins of interhemispheric diaschisis in this case are harder to understand. Presumably, this represents aberrant interactions across two very different time scales. First, the development of interhemispheric connections might be disrupted over a period of weeks. Subsequently, the expression of interhemispheric coordination will be disrupted due to the abnormal connections and the transient abnormal dynamics in one hemisphere that then fails to coordinate adequately with the other. Similarly, periods where large negative correlations are present may be due to degradation in timing mechanisms, also due to the failures of interregional coordination.

Our previous findings suggest that brain incoordination would be reflected in abnormal behavior in rats (Olypher et al., 2006; Wesierska et al., 2005). In the clinical context, we would expect that this incoordination could be reflected in both the cognitive and psychiatric dysfunction sometimes observed in MTLE patients (Bailet and Turk, 2000; Hermann et al., 2009; Oyegbile et al., 2004). Cognitive and psychiatric comorbidities are being increasingly recognized as common phenomena in medial temporal lobe epilepsy (MTLE) and as clinical factors whose quality-of-life impact sometimes exceeds that of the seizures themselves (Gaitatzis et al., 2004; Hermann et al., 2000; Jacoby et al., 2009; Johnson et al., 2004; Oyegbile et al., 2004; Schwartz and Marsh, 2000). Organic etiology for these psychiatric symptoms seems likely, and there are a number of results that suggest ongoing interictal brain abnormalities in the epileptic brain (Hermann et al., 2009). This apparent association between behavioral and psychiatric abnormalities and cognitive disorder in epilepsy complements the growing realization that cognitive deficits may be fundamental in schizophrenia (Hermann et al., 2008; Phillips and Silverstein, 2003).

REFERENCES

Bailet LL, Turk WR. The impact of childhood epilepsy on neurocognitive and behavioral performance: a prospective longitudinal study. *Epilepsia.* 2000; 41:426–431.

Carnevale NT, Hines ML. *The NEURON Book.* New York, NY: Cambridge University Press; 2006.

Costa M, Goldberger AL, Peng CK. Multiscale entropy analysis of complex physiologic time series. *Phys Rev Lett*. 2002;89:68102-1–68102-4.

Feeney DM, Baron JC. Diaschisis. *Stroke.* 1986;17:817–830.

Gaitatzis A, Trimble MR, Sander JW. The psychiatric comorbidity of epilepsy. *Acta Neurol Scand.* 2004;110:207–220.

Goldberger AL, Amaral LAN, Hausdorff JM, et al. Fractal dynamics in physiology: alterations with disease and aging. *Proc Natl Acad Sci USA.* 2002;99: 2466–2472.

Hermann BP, Jones JE, Sheth R, et al. Growing up with epilepsy: a two-year investigation of cognitive development in children with new onset epilepsy. *Epilepsia.* 2008;49:1847–1858.

Hermann BP, Lin JJ, Jones JE, Seidenberg M. The emerging architecture of neuropsychological impairment in epilepsy. *Neurol Clin.* 2009;27:881–907.

Hermann BP, Seidenberg M, Bell B, et al. Comorbid psychiatric symptoms in temporal lobe epilepsy: association with chronicity of epilepsy and impact on quality of life. *Epilepsy Behav.* 2000;1:184–190.

Jacoby A, Snape D, Baker GA. Determinants of quality of life in people with epilepsy. *Neurol Clin.* 2009;27:843–863.

Johnson EK, Jones JE, Seidenberg M, Hermann BP. The relative impact of anxiety, depression, and clinical seizure features on health-related quality of life in epilepsy. *Epilepsia.* 2004;45:544–550.

Kempinsky WH. Experimental study of distant effects of acute focal brain injury; a study of diaschisis. *AMA Arch Neurol Psychiatry.* 1958;79:376–389.

Kramer MA, Kolaczyk ED, Kirsch HE. Emergent network topology at seizure onset in humans. *Epilepsy Res.* 2008;79:173–186.

Lake DE, Richman JS, Griffin MP, Moorman JR. Sample entropy analysis of neonatal heart rate variability. *Am J Physiol Regul Integr Comp Physiol.* 2002;283:789–797.

Li X, Cui S, Voss LJ. Using permutation entropy to measure the electroencephalographic effects of sevoflurane. *Anesthesiology.* 2008;109:448–456.

Lipska BK, Jaskiw GE, Weinberger DR. Postpubertal emergence of hyperresponsiveness to stress and to amphetamine after neonatal excitotoxic hippocampal damage: a potential animal model of schizophrenia. *Neuropsychopharmacology.* 1993;9:67–75.

Lytton WW. Neural query system: data-mining from within the NEURON simulator. *Neuroinformatics.* 2006;4:163–176.

Meyer JS, Obara K, Muramatsu K. Diaschisis. *Neurol Res.* 1993;15:362–366.

Olypher AV, Klement D, Fenton AA. Cognitive disorganization in hippocampus: a physiological model of the disorganization in psychosis. *J Neurosci.* 2006;26:158–168.

Ossadtchi A, Greenblatt RE, Towle VL, et al. Inferring spatiotemporal network patterns from intracranial EEG data. *Clin Neurophysiol.* 2010;121:823–835.

Oyegbile TO, Dow C, Jones J, et al. The nature and course of neuropsychological morbidity in chronic temporal lobe epilepsy. *Neurology.* 2004;62:1736–1742.

Phillips WA, Silverstein SM. Convergence of biological and psychological perspectives on cognitive coordination in schizophrenia. *Behav Brain Sci.* 2003;26:65–82.

Reggia JA, Goodall SM, Shkuro Y, Glezer M. The callosal dilemma: explaining diaschisis in the context of hemispheric rivalry via a neural network model. *Neurol Res.* 2001;23:465–471.

Richman JS, Moorman JR. Physiological time-series analysis using approximate entropy and sample entropy. *Am J Physiol Heart Circ Physiol.* 2000;278: H2039–H2049.

Schwartz JM, Marsh L. The psychiatric perspectives of epilepsy. *Psychosomatics.* 2000;41:31–38.

The MathWorks Inc. MU Guide. Natick, MA: The MathWorks Inc.; 1998.

Uhlhaas PJ, Singer W. Neural synchrony in brain disorders: relevance for cognitive dysfunctions and pathophysiology. *Neuron.* 2006;52:155–168.

Usui N, Terada K, Baba K, et al. Very high frequency oscillations (over 1000Hz) in human epilepsy. *Clin Neurophysiol.* 2010;121:1825–1831.

von Monakow C. Die Lokalisation im Grosshirn und der Abbau der Funktion durch kortikale Herde. Wiesbaden, Germany: JF Bergmann; 1914.

Weber B, Lehnertz K, Elger CE, Wieser HG. Neuronal complexity loss in interictal EEG recorded with foramen ovale electrodes predicts side of primary epileptogenic area in temporal lobe epilepsy: a replication study. *Epilepsia.* 1998;39:922–927.

Wesierska M, Dockery C, Fenton AA. Beyond memory, navigation, and inhibition: behavioral evidence for hippocampus-dependent cognitive coordination in the rat. *J Neurosci.* 2005;25:2413–2419.

White AM, Williams PA, Ferraro DJ, et al. Efficient unsupervised algorithms for the detection of seizures in continuous EEG recordings from rats after brain injury. *J Neurosci Methods.* 2006;152:255–266.

Widman G, Lehnertz K, Urbach H, Elger CE. Spatial distribution of neuronal complexity loss in neocortical lesional epilepsies. *Epilepsia.* 2000;41:811–817.

Zhong J, Chuang SC, Bianchi R, et al. Bc1 regulation of metabotropic glutamate receptor-mediated neuronal excitability. *J Neurosci.* 2009;29:9977–9986.